ChemPubSoc Europe

DOI: 10.1002/slct.201802171

Chemistry SELECT Full Papers

Sustainable Chemistry

Alternative Biofuel Materials for Microbial Fuel Cells from Poplar Wood

Ahmet Erensoy[a] and Nurettin Çek*[b]

In this study, biofuel properties of poplar wood materials rich in organic materials were investigated for microbial fuel cells. Therefore, in this study, investigates the chemical, biochemical properties with electrochemical performance of single chamber microbial fuel cell manufactured using poplar biomass materials, natural soil, graphite anode electrode and graphite cathode electrode. With the increase in the weight of the poplar tree in the microbial fuel cells, the power density increased. SEM, EDS, FTIR analyses showed that *bacillus* and *coccus* type bacteria in the natural structure of the soil act as the catalyst in the anode electrode. Poplar wood, electrodes and bacteria have served in harmony. According to experimental results, the maximum power reaches to 16.88 mW and microbial fuel cell successfully displays a maximum power density of 8555 mW/m^2. All these results indicate that poplar wood may be appropriate biofuel sources for electrical energy generation as an effective environmentally microbial fuel cell technology.

Introduction

Microbial fuel cells are electrochemical systems that convert stored energy in the chemical bonds of organic materials into direct electrical energy through bio-catalytic reactions using microorganisms.[1–6] The electrode materials, the activity of bacteria, biofuel sources (energy sources or substrates) are some of the major factors affecting the electrochemical performances of microbial fuel cells.[2] Briefly, it is important to modify biofuel source for the increment of their electrochemical performances, which may to guidance more efficient microbial fuel cell. Therefore, different types organic materials are used as biofuel sources to obtain high electrical power output in microbial fuel cells. Researches are conducting various studies to find suitable organic biofuel materials. In microbial fuel cell researches most often wastewater, activated sludge, carbohydrates, sugars (glucose, sucrose, etc.) compost and organic substances are in use as a biofuel source.[3–6] Additionally, moss and algae biomasses contain high amount of organic materials that are recently in use as the alternative biofuel material for microbial fuel cells.[7] The potato as a biomass types can be used as a biofuel source for microbial fuel cells.[8] As alternative biofuel material for microbial fuel cells, the use of biomass in various species with high amounts of organic material will become increasingly common. The poplar plant is a forest biomass producing organic nutrients by photosynthesis, and it contains organic material at a good level. The poplar trees include available of glycoside, phenol, acid, cellulose, sugars, etc. organic materials.[9,10] In this study, the poplar tree (wood) is taken into consideration as the biofuel material for microbial fuel cells. Therefore, three different types of microbial fuel cells were produced in which the poplar wood was used as biofuel sources. The properties of the manufactured microbial fuel cell such as chemical, biochemical and electrochemical were examined.

Experimental

Methods

During the study also plastic boxes of 4 cm of bottom diameter, 7 cm of ceiling diameter, 8 cm of diameter are used for the microbial fuel cells. Conductive electrolyte and bacteria catalysts are fundamental elements for the microbial fuel cells. As noted earlier, the natural soil has a conductive structure and is a suitable living space for bacteria[7] and therefore, natural soil use is preferred in this study. Three plastic boxes are adapted with equal quantity of soil (50 grams each). The experimental soil is obtained from Elazığ (Turkey). Box 1, box 2 and box 3 are prepared with poplar wood sawdust of 1%, 10% and 20% of the total soil (by weight), respectively. The poplar plants sawdust are placed in the soil and they are stirred with homogeneous dispersion for 10 minutes. The poplar tree (wood) sawdust in the experiment is the same poplar material, which is formed during poplar tree (wood) cut with the saw. The anode and cathode electrodes (their surface areas 19.73 cm^2) are set between the upper surface (ceiling) and the bottom surface of the plastic boxes. Anode and cathode electrodes are contacted with the soil material mixture including the poplar tree (wood) shavings. Subsequently, 50 mL of water is placed in each box.

[a] *A. Erensoy*
Department of Parasitology, Faculty of Medicine, Fırat University, Elazığ 23119, Turkey
E-mail: aerensoy@firat.edu.tr

[b] *N. Çek*
Department of Metallurgical and Materials Engineering, Engineering Faculty, Fırat University, Elazığ 23119, Turkey
E-mail: nurettincek001@gmail.com

Supporting information for this article is available on the WWW under https://doi.org/10.1002/slct.201802171

© 2018 Wiley-VCH Verlag GmbH & Co. KGaA, Weinheim

Anode and cathode electrodes are connected with the external circuit consisting of conductive wire. Thus, three type single chamber microbial fuel cells were manufactured. As in previous studies, a single chamber microbial fuel cell was preferred because it provides higher electrical power output and low internal resistance than a double chamber microbial fuel cell.[3]

The microbial fuel cell of 1% poplar is referred to the first type microbial fuel cell with the microbial fuel cell containing 10% poplar, and the second type microbial fuel cell as well as the third type microbial fuel cell containing microbial fuel cell of 20% poplar. Three replications are employed in this experiment. Bacterial growth is kept at medium level with constant pH value, chemical pre-treatment etc., everything is examined in the natural process. The electrical and chemical properties of the manufactured microbial fuel cells are also examined leading to the findings that have been explained with the connection principle of causality.

Table 1. Bacteria characteristics and ENA information.

ENA sequence	Bacteria characteristics	Homology
CP014449.1	*Enterococcus faecium strain* ATCC 700221, complete genome	99%
CP011828.1	*Enterococcus faecium strain* UW8175, complete genome	99%
KR054671.1	*Enterococcus faecium strain* GsIIB2212 16 S ribosomal RNA gene, partial sequence	99%
KR054669.1	*Enterococcus faecium strain* GsfIV124 16 S ribosomal RNA gene, partial sequence	99%
KJ571216.1	*Enterococcus faecium strain* TS4E3 16 S ribosomal RNA gene, partial sequence	99%
CP015150.1	*Bacillus thuringiensis strain* Bc601, complete genome	98%
KU179338.1	*Bacillus thuringiensis strain* L26 16 S ribosomal RNA gene, partial sequence	98%
KT720292.1	*Bacillus cereus strain* V20.C2f 16 S ribosomal RNA gene, partial sequence	98%
KT720291.1	*Bacillus cereus strain* V20.C2 16 S ribosomal RNA gene,partial sequence	98%

Results and Discussion

Chemical and Biochemical Analyses

For the soil and water mixture in the experiments, the pH value at 8.00, the total dissolved solid value at 210 mg/L and the salinity at 0.27 psu. These values were obtained from the natural structure of the soil and water mixture. For the soil and water mixture in the experiments, the pH value at 8.00 and the total dissolved solid value at 210 mg/L and the salinity at 0.27 psu. These analyses are made for three types of microbial fuel cells after 6 days. For the first type, microbial fuel cell had pH value at 7.40, the total dissolved solid at 217 mg/L and the salinity at 0.26 psu. The second type microbial fuel cell is measured as pH value at 7.31, the total dissolved solid value at 222.3 mg/L and the salinity at 0.26 psu. Third type microbial fuel cell has measurements as pH at 7.25, the total dissolved solid at 240.9 mg/L and the salinity at 0.26 psu. For all these measurements, the multiparameter instrument is used. According to these results, as the ratio of poplar tree sawdust increases the pH value decreases (pH approached the neutrality), the amount of total dissolved solids increases also with the electrical conductivity, but the salinity value remained the same. According to these results, poplar tree sawdust solution in the soil levies organic and inorganic materials in the soil and soil organic materials ratio improves, with the bacterial activity improvement and chemical reactions continue to be active. Analysis of bacteria in this study was done by 16 S rDNA method and supported by microscope images. In this study, the identified bacteria characteristics and European Nucleotide Archive (ENA) information were given in Table 1.

For microbial analyses a microscope and 16 S rDNA method are used, which provided the most *bacillus* and *coccus* and type bacteria occurrences. These bacteria serves as catalyse poplar wood sawdust. The poplar sawdust is organic material that forms biofuels. Bacteria catalyse the organic poplar wood shavings to release electrons (e^-), protons (H^+) and organic materials. The released electrons go to the anode subsequently go to the external circuit from anode to cathode electrode. The released protons go to the cathode electrode because of the electrolyte. The combination of oxygen (O_2), electrons (e^-) and protons (H^+) from the air provides the water (H_2O) and electrical charge balance. As a result of all these, oxidation reaction for anode and reduction reaction for cathode take place. Thus, the microbial fuel cell produces electrical energy and this status is shown in Figure 1.

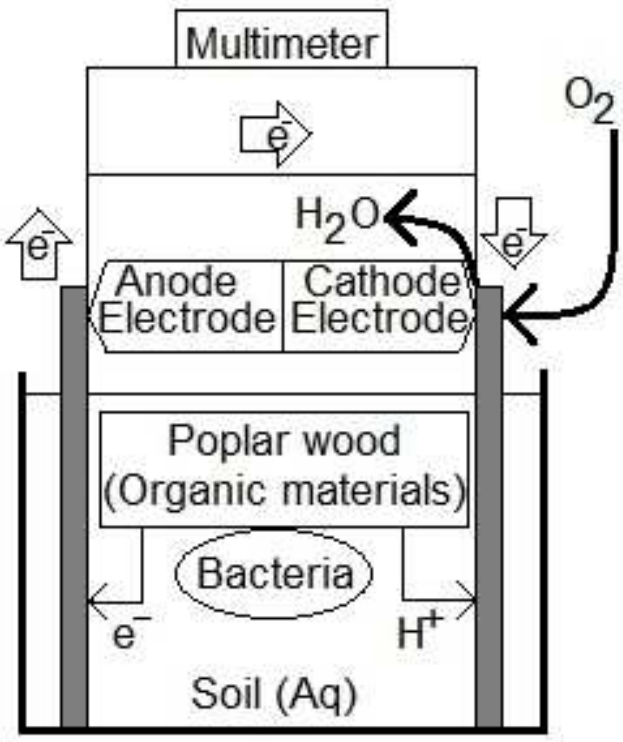

Figure 1. Microbial fuel cell operating system.

© 2018 Wiley-VCH Verlag GmbH & Co. KGaA, Weinheim

Organic materials of poplar tree (wood) sawdust are appropriate to microbial utilization, because they are nutrients for bacteria and they have positive effects on bacterial growth. The release of organic nutrients and their use by bacteria are beneficial for microbial fuel cells and soil, because in this manner soil organic materials content is enriched, and on the other hand, bacterial activity, soil quality and soil efficiency increase. Environmentally and plant friendly microbial fuel cell are manufactured. Due to bacterial activations, a biofilm layer is formed especially on the surface of the anode electrode. Biofilm provides electron transfers to the anode electrode. If there is inert biomass accumulation due to the increase in the thickness of the biofilm layer on the electrode surface, then the performance of the microbial fuel cell decreases.[11] As in the previous studies, to determine the entity of biofilm on the electrode surface, scanning electron microscope (SEM) of the graphite electrodes is used before and after microbial fuel cell work and the results are shown in Figure 2.[11–13]

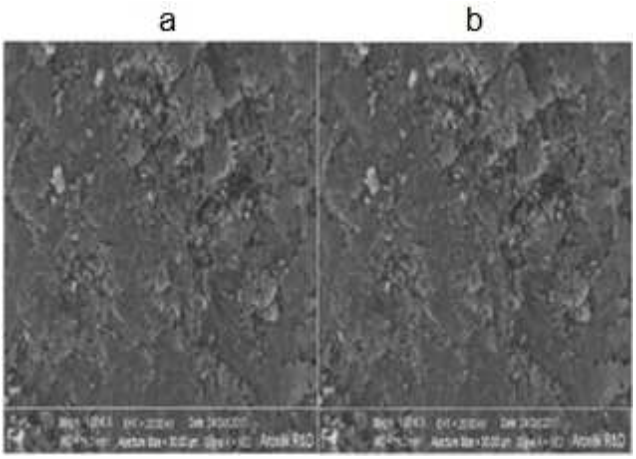

Figure 2. SEM image of graphite electrodes before use. (a) Anode electrode. (b) Cathode electrode.

The elemental analyses of unused graphite anodes, and graphite cathode are equal and their elemental analyses are determined using energy scattered X-Ray spectrometer (EDS) given in Table 2.

Table 2. EDS analysis of unused electrodes.

Element	Unn.C (wt%)	Norm.C (wt%)	Atom.C (wt%)	Sigma (wt%)
Carbon	95.96	96.96	96.94	32.34
Oxygen	4.04	4.04	3.06	2.82

According to Table 2, EDS analysis indicates the graphite usage as the electrodes had the high carbon ratio. This status is proof that graphite electrodes are inert. Furthermore, 6 days throughout SEM images of the used graphite electrodes are shown in Figure 3.

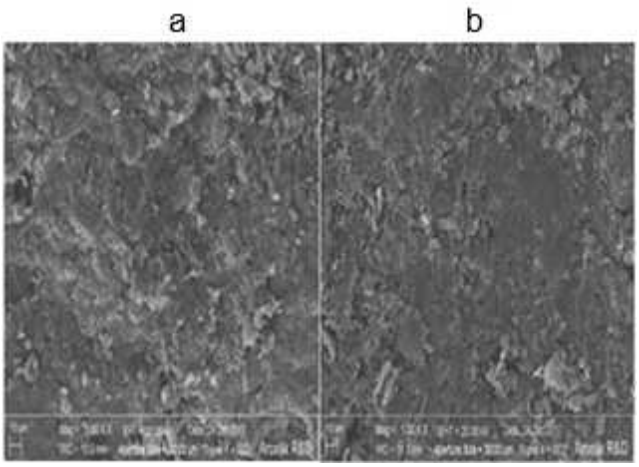

Figure 3. SEM image of used electrodes. (a) Anode electrode. (b) Cathode electrode.

Finally, 6 days throughout EDS analyses of the used graphite electrodes are given in Table 3.

Table 3. EDS analysis of used electrodes.

	Anode electrode		Cathode electrode	
	Carbon	Oxygen	Carbon	Oxygen
Unn.C (wt%)	94.71	5.29	95.68	4.32
Norm.C (wt%)	94.71	5.29	95.68	4.32
Atom.C (wt%)	95.97	4.03	96.72	3.28
Sigma (wt%)	31.88	3.36	32.30	2.97

According to Tables 2 and 3, a lower carbon ratio and a higher oxygen ratio are detected in the anode graphite electrode than in the cathode electrode. This situation indicates that the oxidation reaction has taken place by the bacteria on the anode graphite electrode. Oxygen is detected in the cathode electrode with a higher quantity than in the unused cathode electrode. Cathode graphite electrode supplied the oxygen needed for the reaction from the air. Due to the reduction reaction, the carbon and oxygen reacted on the graphite cathode electrode, low ratio carbon dioxide is revealed, and therefore, carbon ratio in the cathode electrode decreases. As in the previous studies, graphite electrodes are modelled by Fourier-transform infrared spectroscopy (FTIR) before and after microbial fuel cell applications which are shown in Figure 4.[12,13]

Similar to the previous studies, the broad band in the 3500–3300 cm^{-1} range is attributed to the free and bound O–H and N–H groups, which could form hydrogen bonding with the carbonyl group of the peptide linkage in the protein. The bands at 2919 cm^{-1} and 2850 cm^{-1} can be attributed to the functional groups of membrane fatty acids and by some amino acid side-chain vibrations, due to the characteristic C–H stretching vibrations of $-CH_3$ and $=CH_2$ functional groups dominate. The band between 2240 and 2280 cm^{-1} attributed

© 2018 Wiley-VCH Verlag GmbH & Co. KGaA, Weinheim

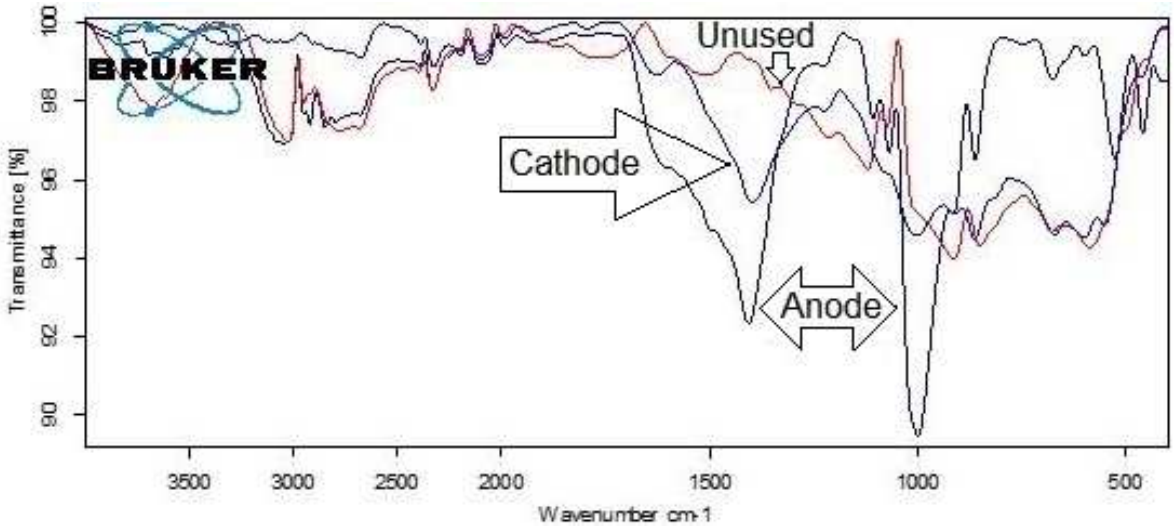

Figure 4. FTIR analyses of electrodes

to (-C: N) nitrile groups of anode electrode. Furthermore, 1538.99 cm^{-1} and 1578.44 cm^{-1} range is characteristic of amide II bands. The band at 1466.29 cm^{-1} is C–H deformation of $=CH_2$ functional groups,[12] and the band 1300–900 cm^{-1} indicates the presence of polysaccharides and nucleic acids.[13] Inert biomass accumulation performance reduction in the microbial fuel cell causes increase in internal resistance of microbial fuel cell. This status reduces the electrical performance. These results confirm the presence of biofilm on the surface of anode graphite electrode. The change of pH values, total dissolved solid increase, SEM analysis, EDS analysis, FTIR analysis, etc. are evidence of bacterial activities and chemical reaction processes. Furthermore, these issues give insights into electrical performances of microbial fuel cells.

Electrochemical Performance of the Developed Microbial Fuel Cells

Primarily for the soil and water mixtures in the experiments electrical conductivity is about 530 μS/cm, which is another proof that the mixture of soil and water function as an electrolyte. The electrical conductivities of microbial fuel cells are measured immediately, and hence, electrical conductivities are equal to each other at 530 μS/cm. After 6 days, the microbial fuel cell electrical conductivities are measured, and their electrical conductivities as appeared as 535.3 μS/cm for the first type microbial fuel cell, 542 μS/cm for the second type and 601.9 μS/cm, for the third type. The multi parameter instrument is used for all these measurements. Microbial fuel cells generate direct current (DC) electricity. Their open-circuit voltage (Voc) and short-circuit current (Isc) values are also measured by the same multimeter. These measurements are on daily basis. In this study, the open-circuit voltage is considered as millivolt (mV) and the short-circuit current as microampere (μA). These measurements are given in Table 4.

Table 4. Time dependent Isc and Voc values of microbial fuel cells.

Time (Day)	First type microbial fuel cell Voc (mV)	Isc (μA)	Second type microbial fuel cell Voc (mV)	Isc (μA)	Third type microbial fuel cell Voc (mV)	Isc (μA)
1	8.6	0.4	3.6	0.3	4.7	0.3
2	4.8	0.4	6.6	0.7	7.7	0.7
3	9.7	2.5	16	1.6	5.6	0.3
4	19.8	1.5	12.5	1.6	5.8	0.5
5	19.8	1.5	30	1.5	51	2.2
6	19.8	1.5	30	1.5	51	2.2

According to Table 4, microbial fuel cells produce the irregular voltage (Voc) and irregular current (Isc) at low values, as in other fuel cell types.[14] The electrical performance of the microbial fuel cells by the polarization curve provides the highest power generation. Fixed short-circuit current and fixed open-circuit voltage are obtained for Microbial fuel cells and after, and their polarization curve works. These curves were designed by using external resistances from 10 to 221500 ohm (Ω) and ensuring appropriate time for voltage balancing at each resistance.[4,6, 8] Polarization curves of microbial fuel cells are shown in Figure 5.

According to this figure, the microbial fuel cell power curves are similar to those of other studies.[5,15, 17] Behind linear adjustment of the polarization curves, the internal resistances of the first, second and third type microbial fuel cell are calculated as 11559 Ω, 29459 Ω, and 26260 Ω, respectively. The internal resistance of a microbial fuel cell consists of three factors, namely, ohmic, activation and diffusion (concentration) resistances.[15–17] Ohmic resistance is determined on the basis of electrolyte type, electrode properties and membrane factors. Since no membrane is used in this study, ohmic resistance is caused from electrode and electrolyte. The resistance of the soil-water mixture has an electrolyte at 1060.9 Ω. Microbial fuel cell electrolytes contain poplar wood sawdust at different rates,

© 2018 Wiley-VCH Verlag GmbH & Co. KGaA, Weinheim

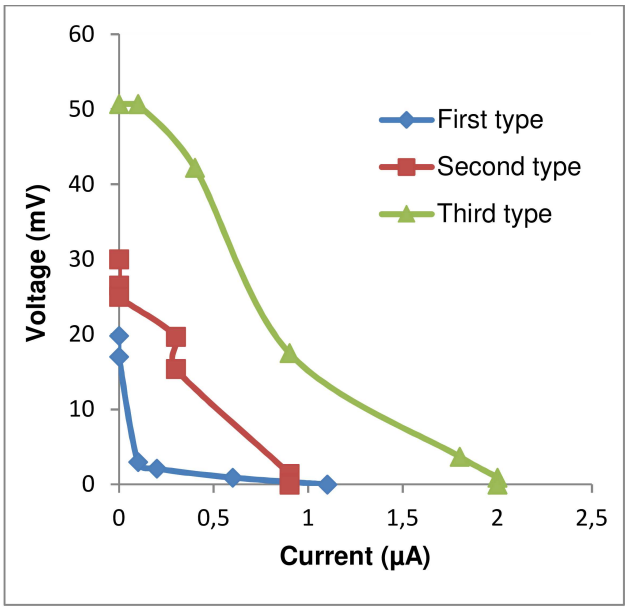

Figure 5. Polarization curves of microbial fuel cells

and therefore, each microbial fuel cell has different resistances. According to measurements after 6 days, the electrolyte resistances of the first, second and third type microbial fuel cell are 1040 Ω, 953.3 Ω and 933 Ω, respectively. Briefly, the third type microbial fuel cell with higher ratio poplar wood sawdust has a higher organic acid content, a higher minerals content, higher total dissolved solid content, a lower low pH value and lower ohmic resistance. Activation resistance by the low speed of the reactions takes place on the surface of the electrode. It is reduced by bacterial activity increase for the anode oxidation reactions and by increase in the activity of the reduction reactions for the cathode.[16,17]

Microbial fuel cells have bacterial activity and reduction reactions as seen in SEM and EDS analyses. Therefore, their activation resistances are also available.

Diffusion (concentration) resistance by the diffusion rate of reaction products is transferred to the electrode surface and electrolyte.[15–18] In order to reduce the diffusion resistance, the inert biomass accumulation in the electrodes must be decreased with the high-performance transfer of the electrons to the anode electrode, protons and oxygen to the cathode electrode.[11][15–19] As can be seen from the FTIR analysis, non-conductive inert materials (CH_3, CH_2, etc. organic materials) are present on the electrode surfaces. In this study, microbial fuel cells have diffusion resistance. All of these internal resistance factors reduce the output voltage and the output voltage (V) according to equation (1).[15]

$$V=E\text{-}Vact\text{-}Vcon\text{-}Vohm \quad (1)$$

where E is the Nernst voltage (thermodynamic potential), Vact is activation voltage, Vcon is concentration overvoltage, and Vohm is ohmic overvoltage.

In this study, all internal resistance factors that cause the voltage drop are active and this is a normal status. There are more or less internal resistance problems in all microbial fuel cells, which are the biggest obstacles to the development and their higher power output of microbial fuel cells. Based on the polarization curves, power (P) values are calculated using equation (2).[20]

$$P=IxV \quad (2)$$

where P is the power (Watt), V is cell voltage, I is cell current. Drawing the power values according to the current values revealed the power curve. The highest point of this curve is the maximum power output values of the cell. Based on equation (2) and polarization curves, the power curves of the microbial fuel cells in this study are presented in Figure 6.

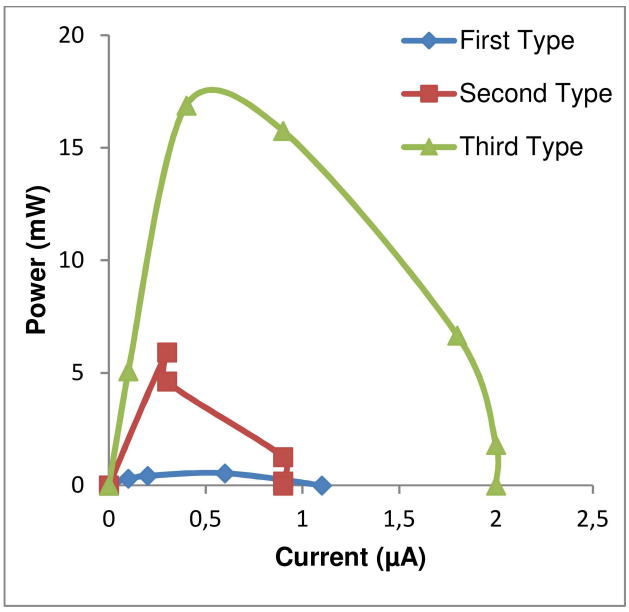

Figure 6. Power curves of microbial fuel cells

According to Figure 6, the power curves of microbial fuel cells are similar to previous studies.[5,17] According to Figure 5, the maximum power output values of first, second and third type microbial fuel cell are calculated as 0.54 mW, 5.91 mW, and 16.88 mW, respectively.

The differences in maximum power density proved the importance of the poplar wood sawdust quantity as a fuel source for electricity generation at microbial fuel cells. According to power curves, power density is calculated according to equation (3).[20]

$$Pdensity = P/A \quad (3)$$

where P is the power (mW), A is anode surface area (m^2).

© 2018 Wiley-VCH Verlag GmbH & Co. KGaA, Weinheim

According to equation (3), the power density 1 values of first, second and third type microbial fuel cell are calculated to as 273 mW/m^2, 2995 mW/m^2, and 8555 mW/m^2, respectively.

The environmental and electrochemical abilities of the third type microbial fuel cell are highly developed, and therefore, it generates high power density according to many microbial fuel cell types.

Summary and Literature Review

Poplar tree (wood) sawdust serves as the alternative biofuel (energy) source for microbial fuel cells.

It is probable that the first type microbial fuel cell rapidly tends to electrical power drop due to the low ratio (1%) organic poplar tree (wood) sawdust quantity.

As the proportion of organic poplar sawdust material increases in the microbial fuel cell, the power output of the microbial fuel cell increases, and therefore, power output reaches the highest level in the third type microbial fuel cell (high organic materials ratio (20%)). Hence, an increase in the amount of organic material improves bacterial activity. All these factors affect the electrical performance of microbial fuel cells. Microbial fuel cells generate electrical power at different values.

Table 5 compares some results for microbial fuel cells with reported power values and biofuel (energy) source with the literature.

As in Table 5, the microbial fuel cell generates electrical energy at higher power. The poplar tree (wood) sawdust in the microbial fuel cell system has more efficiency rather than the other biofuel (energy) sources.

Table 5. Literature summary and comparison

Biofuel (Energy) Source	Anode Electrode	Cathode Electrode	Max. Power (mW/m^2)	Ref.
Potato + Sludge	Carbon felt	Carbon felt	6.8	[8].
Waste-water	Carbon brush	Carbon felt	7.9	[13].
Moss	Zinc	Copper	17.6	[7].
Moss	Zinc	Copper	18.24	[7].
Waste-water	Carbon felt	Carbon felt	22	[12].
Organic matters	Carbon felt	Carbon felt	32	[1].
Glucose	Carbon cloth	Carbon cloth	44.2	[19].
Activated-sludge	Carbon paper	PTFE	52	[4].
Organic matters	Carbon fiber brush	Carbon fiber brush	391	[16].
Compost soil	Zinc	Graphite	5335.5	[20].
Poplar sawdust	Graphite	Graphite	8555	This study

Conclusion

Poplar tree sawdust based on microbial fuel cell is advantageous due to its high power output environmentally with simplified manufacturing properties. In addition, it is demonstrated the first time that the use of poplar tree (wood) sawdust as biofuel materials are effective in the microbial fuel cell applications. In order to fully obtain sustainability with higher efficiency it is necessary to base on bacteria feeder organic materials that are able to conduct the microbial activity. Electrical energy generation has been handled using the proposed microbial fuel cell while respecting the internal resistance to the high power density, DC voltage, electrodes, bacterial activity, organic materials, etc., factors. The proposed microbial fuel cell system can achieve rejoicing performance when optimum parameters are chosen and suitable materials are used, and therefore, this can be applied for electrical-electronic systems. In addition, the use of computer-aided electronic systems is increasing day by day, and therefore, electricity needs are increasing. After, all environment friendly energy production systems are valid by microbial fuel cells, electric-electronic and computer-aided systems.

Supporting Information Summary

Used materials, detailed experiment apparatus and instruments.

Acknowledgements

We especially appreciate the help from Koç Holding, Arçelik and Tüpraş for the experimental instruments.

Conflict of Interest

The authors declare no conflict of interest.

Keywords: biomass · environment friendly energy · microbial fuel cell · poplar

[1] S. Aslan, P. O'Conghaile, D. Leech, L. Gorton, S. Timur, U. Anik, *ChemistrySelect.* **2017**, *2*, 12034–12040.
[2] S. Aslan, P. O'Conghaile, D. Leech, L. Gorton, S. Timur, U. Anik, *Electroanalysis.* **2017**, *29*, 1651–1657.
[3] SJ. You, QL. Zhao, JQ. Jiang, J. N. Zhang, SQ. Zhao, *J. Environ. Sci. Health., Part A.* **2006**, *41*, 2721–2734.
[4] D. Khater, KM. El-khatib, M. Hazaa, RYA. Hassan, *J. Bas. &Environ. Sci.* **2015**, *2*, 63–73.
[5] N. Çek, Parçacıklar ve Enerji Kaynakları. 1nd ed. Saarbrucken, Germany: Lambert Academic Publishing, **2016**.
[6] V. Chaturvedi, P. Verma, *Bioresour. Bioprocess.* **2016**, *3*, 1–14.
[7] N. Çek, Biofuel cell design with moss. In: 10th International Clean Energy Symposium; 24–26 October **2016**; İstanbul, Turkey. pp. 182–193.
[8] H. Du, L. Fusheng, *J. Cleaner Prod.* **2017**, *143*, 336–344.
[9] P. Ristivojević, J. Trifković, F. Andrić, D. Milojković-Opsenica, *Nat. Prod. Commun.* **2015**, *10*, 1869–1876.
[10] RK. Devappa, SK. Rakshit, RFH Dekker, *Biotechnol. Adv.* **2015**, *33*, 681–716.
[11] AK. Marcus, CI. Torres, BE. Rittmann, *Biotechnol. Bioeng.* **2007**, *98*, 1171–1182.
[12] E. Baranitharan, MR. Khan, DM. Prasad, WF. Teo, GY. Tan, R. Jose, *Bioprocess Biosyst. Eng.* **2015**, *38*, 15–24.
[13] MA Islam, A Karim, CW Wai, B Ethiraj, CK Cheng, A Yousuf, MMR Khan, *RSC Adv.* **2017**, *7*, 4798–4805.
[14] S. Salehi, B. Vahidi, JM. Monfared, M. Taheri, H. Moradi, *Turk J Elec Eng & Comp Sci.* **2015**, *23*, 2182–2196.

© 2018 Wiley-VCH Verlag GmbH & Co. KGaA, Weinheim

[15] M. Valizadeh, MR. Feyzi, E. Babaei, M. Sabahi, *Turk J Elec Eng & Comp Sci.* **2015**, *23*, 317–334.
[16] H. Tursun, R. Liu, J. Li, R. Abro, X. Wang, Y. Gao, Y. Li, *Front. Microbiol.* **2016**, *7*, 1–9.
[17] BE. Logan, B. Hamelers, R. Rozendal, U. Schröder, J. Keller, S. Freguia, P. Aelterman, W. Verstraete, K. Rabaey, *Environ. Sci. Technol.* **2006**, *40*, 5181–5192.
[18] G. Gupta, B. Sikarwar, V. Vasudevan, M. Boopathi, O. Kumar, B. Singh, R. Vijayaraghavan, *J. Cell Tissue Res.* **2011**, *11*, 2631–2654.
[19] C. Li, L. Zhang, M. Xu, L. Ding, K. Xu, J. Geng, H. Ren, *Asian J. Chem.* **2013**, *25*, 4165–4170.
[20] N. Çek, *GU J Sci.* **2017**, *30*, 395–402.

Submitted: July 11, 2018
Accepted: October 17, 2018

© 2018 Wiley-VCH Verlag GmbH & Co. KGaA, Weinheim